Received: 17 October 2019 | Revised: 29 January 2020 | Accepted: 27 February 2020 | Published on: 1 April 2020

DOI: 10.1002/qj.3779

Quarterly Journal of the Royal Meteorological Society RMetS

RESEARCH ARTICLE

Probabilistic high-impact rainfall forecasts from landfalling tropical cyclones using Warn-on-Forecast system

Nusrat Yussouf[1,2,3] | Thomas A. Jones[1,2,3] | Patrick S. Skinner[1,2,3]

[1]Cooperative Institute for Mesoscale Meteorological Studies, University of Oklahoma, Norman, Oklahoma

[2]NOAA/OAR/National Severe Storms Laboratory, Norman, Oklahoma

[3]School of Meteorology, University of Oklahoma, Norman, Oklahoma

Correspondence
N. Yussouf, NOAA/National Severe Storms Laboratory National Weather Center, 120 David L. Boren Boulevard, Norman, OK 73072, USA.
Email: nusrat.yussouf@noaa.gov

Funding information
NOAA-University of Oklahoma Cooperative Agreement #NA11OAR4320072, U.S. Department of Commerce., Grant/Award Number: NA11OAR4320072

Abstract

Intense rainfall and flash flooding from landfalling tropical cyclones (LTC) can have devastating impacts on human life and property in coastal areas. The years 2017 and 2018 are examples of how the North Atlantic LTCs can create widespread destruction in the United States. Better preparedness is needed to mitigate the impact from the violent LTCs and can be achieved by improving the accuracy of forecasts and increased lead-time of guidance products. However, predicting the fine-scale details of rain bands in LTC is very challenging. This study attempts to elucidate the potential of National Severe Storms Laboratory's convective-scale ensemble analysis and prediction system, known as the Warn-on-Forecast System (WoFS), in improving 0–6 hr probabilistic intense rainfall forecasts from three recent LTCs in the United States. Results indicate that the frequent 15 min assimilation cycling can accurately analyse the small-scale details from the LTC rain bands in the WoFS analyses. The WoFS 0–6 hr ensemble forecasts initialized from those analyses represent the location, intensity and spatial distribution of intense rainfall (with the potential to cause flash flooding) as well as low-level rotation with reasonably good accuracy. The continuous flow of the frequently updated WoFS rainfall guidance has the potential to aid operational forecasters in issuing watches, warnings, and short-term forecast products of life-threatening LTC with higher spatial and temporal specificity.

KEYWORDS

convective-scale numerical modelling, ensemble data assimilation, ensemble forecasting, intense rainfall and flash flood, landfalling tropical cyclones

1 | INTRODUCTION

There is an increase in vulnerability to the hazards associated with landfalling tropical cyclones (LTCs) due to rapid development of infrastructure and rise in population growth along the coastal regions of the world (e.g. Pielke Jr and Pielke Sr, 1997; Rappaport, 2000; Peduzzi *et al.*, 2012; Rappaport and Blanchard, 2016; Klotzbach *et al.*, 2018). The combined effects of localized extreme wind, intense rainfall, flash flooding, and storm surges from LTCs are a leading cause of economic damage in the USA (Aon Benfield, 2019) and other countries (Leroux *et al.*, 2018). The destructive 2017 North Atlantic hurricane season alone resulted in damage worth ~$125 billion in the USA (Aon

Benfield, 2018). Actionable protective decisions during these types of phenomena depend on accurate prediction and early warning of the location, timing, and intensity of the localized weather threats. Recognizing the critical importance of prioritizing global weather research on improving the forecast accuracy and communicating this high-impact weather from minutes to 2 weeks, the World Meteorological Organization's World Weather Research Programme established the HIWeather[1] project (WMO, 2017).

While most of the LTC weather warnings issued are focused on extreme localized winds, heavy precipitation from LTC rain bands often results in serious flooding and flash flooding which is responsible for a large number of fatalities and economic damage worldwide (e.g. Jonkman *et al.*, 2009; Czajkowski *et al.*, 2011; 2013; Dare *et al.*, 2012; Meyer *et al.*, 2014). About 27% of all the North Atlantic LTC fatalities over the period 1963–2012 were related to heavy rainfall and flooding (Rappaport, 2014). The devastating impact from intense LTC rainfall (Blake and Zelinsky, 2018; Beven *et al.*, 2019; Stewart and Berg, 2019) can be reduced by improving the accuracy and lead-time of National Weather Service (NWS) flash flood and rainfall forecasts. Early watches and warnings with high temporal and spatial specificity will give stakeholders adequate time to take action. However, forecasting the small-scale details of the rainfall distribution within the LTC rain bands is still a challenge (e.g. Atallah *et al.*, 2007; Zhang *et al.*, 2010) despite recent advances in data assimilation (DA) and numerical weather prediction (NWP) modelling (Alley *et al.*, 2019). Most of the NWP modelling studies conducted so far have focused on improving the hurricane track and intensity forecasts (e.g. Aksoy *et al.*, 2013; Zhang and Weng, 2015; Lu *et al.*, 2017; Tong *et al.*, 2018; Zhang *et al.*, 2019). With the likely rapid increase in the occurrence of extreme hurricane rainfall during the twenty-first century (Emanuel, 2017), it is crucial to provide forecasters with accurate and skilful model guidance with finer temporal and spatial details. The convective-scale processes responsible for extreme LTC rainfall are inherently nonlinear and therefore highly sensitive to uncertainties in physical processes and initial and boundary conditions. These sensitivities motivate the use of an ensemble approach at convection-permitting resolution (Zhang and Weng, 2015). With the exponential increase in supercomputer power in recent years, running convective-scale ensembles to represent uncertainties in the forecasts of hazardous weather events is a reality.

The National Oceanic and Atmospheric Administration (NOAA) National Severe Storms Laboratory's (NSSL's) Warn-on-Forecast programme (Stensrud *et al.*, 2009; 2013) is developing and testing an on-demand, regional, cycled, convective-scale, ensemble-based prediction system, known as the Warn-on-Forecast System (WoFS). The WoFS is designed to provide continuous, 0–6 hr probabilistic model guidance of high-impact weather threats (for example, low-level rotation, intense rainfall, flash flooding, extreme winds, and large hail) from individual convective storms (e.g. Yussouf *et al.*, 2013a; 2013b; 2015; 2016; Wheatley *et al.*, 2015; Jones *et al.*, 2016; 2018; Skinner *et al.*, 2016; 2018; Yussouf and Knopfmeier, 2019). The goal of the WoF programme is to aid NWS forecast centres, such as the Storm Prediction Center (SPC) and the Weather Prediction Center (WPC), and local forecast offices in filling the gap in NWP guidance (Stensrud *et al.*, 2009; Rothfusz *et al.*, 2018) of hazardous weather on current watch-to-warning time-scales. Until recently, the WoFS has been applied to midlatitude spring and summertime hazardous convective weather; however, the system that is being developed can be applied to predict hazards associated with LTCs. Jones *et al.* (2019) demonstrated the capability of WoFS in predicting extreme localized winds and tornado potential within LTCs. This study assesses the ability of WoFS in predicting extreme rainfall that often led to widespread flash flooding in three recent LTCs in the United States, namely Hurricanes *Harvey* (2017), *Florence* (2018) and *Michael* (2018). The WoFS was run in retrospective mode for *Harvey* and forecasts generated in real-time are examined for hurricanes *Florence* and *Michael*. An overview of the three LTCs is given in Section 2. The experimental WoFS configuration is described in Section 3. Section 4 discusses the ensemble forecasts. A summary and concluding remarks are provided in Section 5.

2 | OVERVIEW OF THE LANDFALLING TROPICAL CYCLONE EVENTS

2.1 | Hurricane *Harvey*

Harvey is the second-most costly hurricane in US history behind only *Katrina* (2005) with a damage estimate of $125 billion. Hurricane *Harvey* approached the middle Texas coast as a category 3 on the Saffir–Simpson scale (Simpson and Riehl, 1981) by noon on 25 August 2017 and rapidly intensified into a category 4 prior to landfall (Figure 1a). *Harvey* made landfall near Rockport, Texas at 0300 UTC 26 August 2017 (Table 1), then rapidly weakened to a tropical storm within 12 hr after landfall. The system slowed considerably and dropped historic amounts of rainfall during the next 4 days. These rains caused catastrophic flooding in the Greater Houston region and over southeastern Texas

[1] http://hiweather.net/

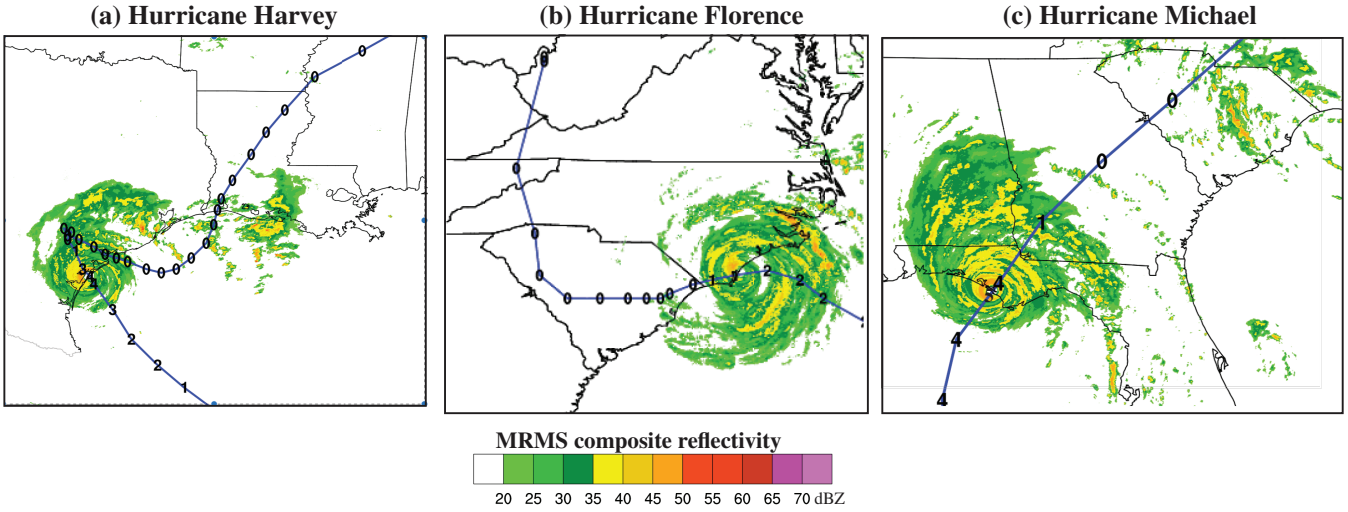

FIGURE 1 Multi-radar multi-sensor (MRMS) composite reflectivity at the time of landfall for hurricanes (a) *Harvey* (26 August 2017 at 0300 UTC), (b) *Florence* (14 September 2018 at 1115 UTC), and (c) *Michael* (10 October 2018 at 1730 UTC). The storm track (black lines) is overlaid with hurricane category on Saffir–Simpson wind scale [Colour figure can be viewed at wileyonlinelibrary.com]

TABLE 1 The name of the three North Atlantic landfalling tropical cyclones (LTC) used in this study with the timing, location and hurricane category at landfall over United States coasts

Name	Date and time of landfall	Landfall location	Hurricane category at landfall on Saffir–Simpson wind scale
Harvey	0300 UTC, 26 August 2017	Gulf Coast, Middle Texas	4
Florence	1100 UTC, 14 September 2018	Southeast Coast, North Carolina	1
Michael	1730 UTC, 10 October 2018	Gulf Coast, Florida Panhandle	5

and resulted in at least 68 direct deaths in Texas. Over 300,000 structures were flooded in that region with up to 500,000 cars reported flooded, and an estimated 40,000 flood victims were evacuated across Texas or Louisiana. Details of Hurricane *Harvey* can be found in Blake and Zelinsky (2018).

2.2 | Hurricane *Florence*

Hurricane *Florence* was a long-lived category-4 hurricane that weakened to category 1 as it approached the southeastern coast of North Carolina (NC; Table 1) and made landfall around 1100 UTC 14 September 2018 (Figure 1b). After landfall, *Florence* moved slowly towards the west-southwest and gradually weakened. The slow forward speed of *Florence* prior to and after landfall resulted in persistent rain bands moving inland off the Atlantic Ocean and trained on the same area in NC. *Florence* produced more than 10 in of rain across much of southeastern and south-central NC, as well as northeastern South Carolina (SC). The highest rainfall totals exceeding 20 in from the NC-SC border eastward across southeastern NC, especially along and to the right of the track of the centre. These excessive rains resulted in extensive low-land and river flooding across much of southeastern and south-central NC and northeastern SC. *Florence* caused 22 direct deaths in the USA. Additional details about this event are provided in Stewart and Berg (2019).

2.3 | Hurricane *Michael*

Michael was a category-5 hurricane that made a catastrophic landfall around 1730 UTC 10 October 2018 (Figure 1c) in the Florida Panhandle, producing devastating winds and storm surge near the coast, and rain and wind inland (Table 1). *Michael* rapidly weakened after landfall as it accelerated northeastward across the central Florida Panhandle with category-3 intensity before the eye moved into southwestern Georgia (GA) around 2130 UTC 10 October. The cyclone weakened to a tropical

storm, continuing northeastward and moved into SC near 1100 UTC 11 October. However, tropical storm-force winds continued over the coastal areas and coastal waters of GA and SC. It was directly responsible for 16 deaths and about $25 billion in damage in the USA. *Michael*'s track across the southeastern USA resulted in widespread rains of 3 to 6 in and localized rainfall totals in excess of 10 in. Details regarding Hurricane *Michael* are documented in Beven *et al.* (2019).

3 | WOFS EXPERIMENT CONFIGURATION

The WoFS uses the Advanced Research Weather Research and Forecasting (WRF-ARW version 3.8.1: Skamarock *et al.*, 2008) model and the Community Gridpoint Statistical Interpolation (GSI: Kleist *et al.*, 2009; DTC, 2017a) based Ensemble Kalman filter (EnKF: Houtekamer *et al.*, 2005; Whitaker *et al.*, 2008; DTC, 2017b) DA (GSI-EnKF) system. The current real-time configuration of WoFS runs at 3 km horizontal grid spacing and uses the experimental High-Resolution Rapid Refresh Ensemble (HRRRE: Dowell *et al.*, 2016) for initial and boundary conditions. The WoFS is a 36-member, multiphysics ensemble with diversity in planetary boundary layer and radiation physics schemes. All ensemble members utilize the NSSL 2-moment microphysics parametrization (Mansell *et al.*, 2010) and the Rapid Refresh (RAP) land-surface model (Smirnova *et al.*, 2016). The placement of the WoFS domain depends on where the hazardous weather is anticipated and is driven by NWS WPC's Day 1 Excessive Rainfall Outlook (EROs). The EROs are issued daily at scheduled intervals as part of WPC's Day 1–3 quantitative precipitation forecasting (QPF) product suite to forecast the probability of exceeding NWS flash flood guidance (FFG[2]: Clark *et al.*, 2014) within 40 km of a point over the contiguous United States. The Day 1 EROs use probability contours of 5% (marginal), 10% (slight), 20% (moderate) and 50% (high) to convey the risk. The WPC issued moderate (MOD) risks for the Day 1 EROs for Hurricane *Harvey* (Figure 2a) and *Michael* (Figure 2b) and high (HIGH) risk for *Florence* (Figure 2c). The corresponding WoFS grids are centred over the risk areas (Figure 2d,e,f). The WoFS experiment for Hurricane *Harvey* was conducted in research mode and therefore a larger domain size was computationally feasible compared to the other two cases. The Multi-Radar Multi-Sensor (MRMS: Smith *et al.*, 2016) reflectivity, Level II radial velocity data from the WSR-88D (indicated by the blue dots in Figure 2d,e,f), and conventional observations (if available) from National Centers for Environmental Prediction (NCEP) are assimilated in WoFS using 15 min cycling frequency. The continuous every 15 min DA cycle enables WoFS to assimilate most recent atmospheric observations, and thus enables the system to accurately analyse convective-scale details in the initial conditions (Figure 3). The 0–6 hr ensemble forecasts are made on the hour with forecast files every 5 min generated (Figure 3) for the three events, and details are listed in Table 2.

[2]The FFG products, which are the estimate of rainfall necessary to cause rivers and small streams to overflow their natural banks, are issued every 6 hr each day.

4 | RESULTS AND DISCUSSION

4.1 | LTC rain bands

WoFS analyses near landfall time generally reproduce accurate representations of the overall inner core (eyewall and eye) and rain band characteristics of each hurricane when comparing model-simulated composite reflectivity (maximum reflectivity from any of the reflectivity angles of the WSR-88D weather radar) against MRMS observations (Figures 1 and 4). For *Harvey*, the strong eyewall convection along the Texas (TX) coast is evident coupled with an extensive rain band farther east. The analysed eyewall characteristics are accurate, though the intensity and coverage of convection along the upper TX and Louisiana (LA) coasts appears to be somewhat over-forecast (Figures 1a and 4a,d). In the case of *Florence*, fewer strong convective cells (reflectivity >45 dbZ) are present and the eyewall is less evident (Figure 4b,e). By this time, *Florence* had weakened significantly from its peak intensity and strong eyewall convection had become less evident. Finally, hurricane *Michael* was also well analysed with a strong eyewall and rain band convection evident (Figure 4c,f). In all cases, analysed reflectivity overestimates the coverage of reflectivity greater than 20 dBZ to some extent. The reflectivity biases are very sensitive to the selection of the microphysics scheme and the parameters within each microphysics scheme. Tuning of the NSSL 2-moment microphysics scheme, which was originally developed for continental convection, is needed for tropical convection. Note that the overall size of *Harvey* is much smaller than either *Florence* or *Michael*, but is also the slowest moving, which significantly increases its threat of heavy precipitation.

The ensemble 0–6 hr forecasts of WoFS composite reflectivity initiated near landfall time show that WoFS has the capability to generate reasonably accurate short-term forecasts of LTC characteristics from the analyses described above. Figure 5 shows the probability of WoFS composite reflectivity greater than 20 dBZ at landfall

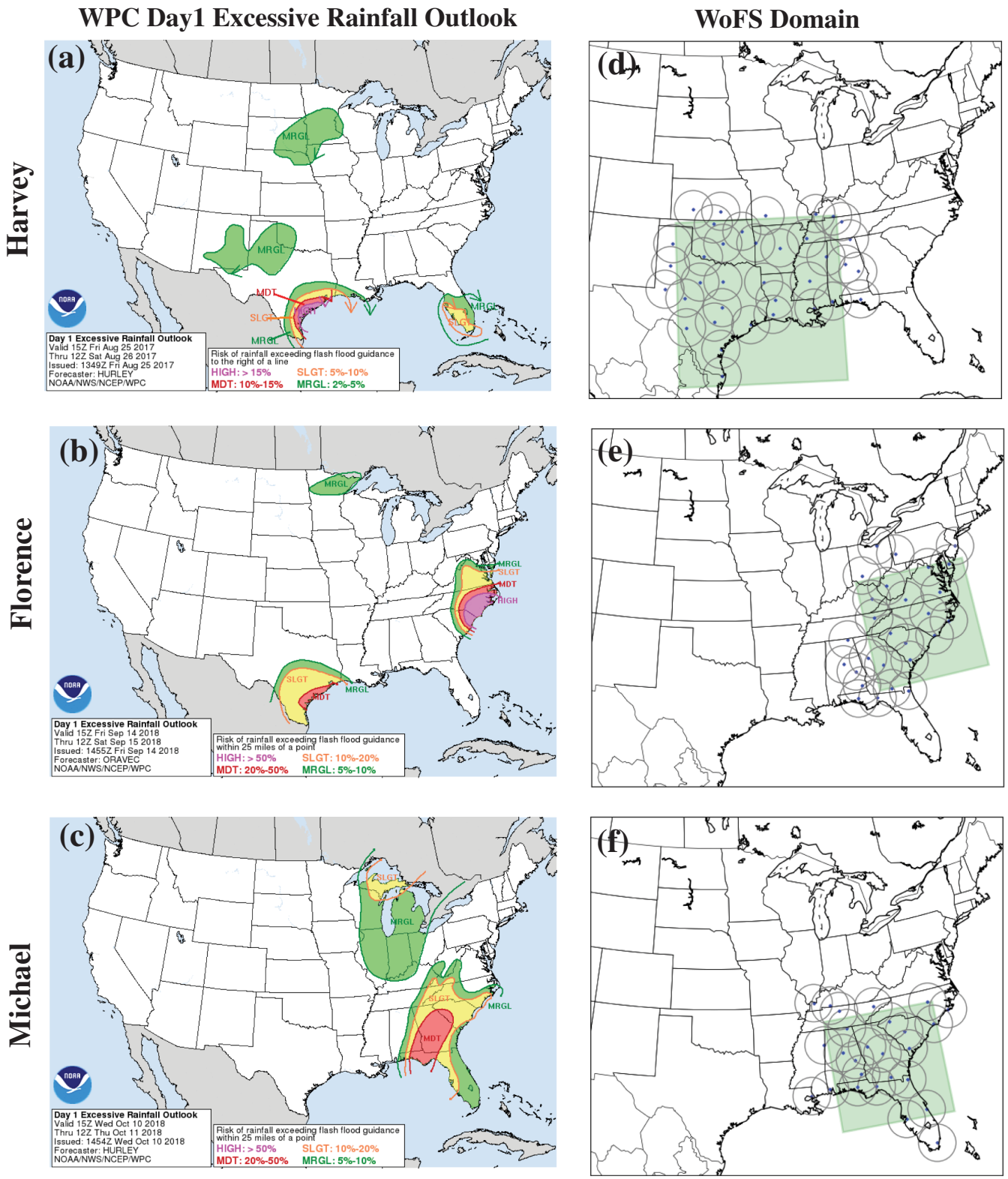

FIGURE 2 Weather Prediction Center's day-1 excessive rainfall outlook (ERO) and the map of the WoFS domains (shaded light green) nested within the HRRRE background for hurricanes (a,d) *Harvey*, (b,e) *Florence*, and (c,f) *Michael*. The ERO risk categories are MRGL (marginal), SLGT (slight), MDT (moderate) and HIGH (high). The locations of WSR-88D within the WoFS grid are shown in blue dots with 150 km range rings and the observations from those radars are assimilated in WoFS [Colour figure can be viewed at wileyonlinelibrary.com]

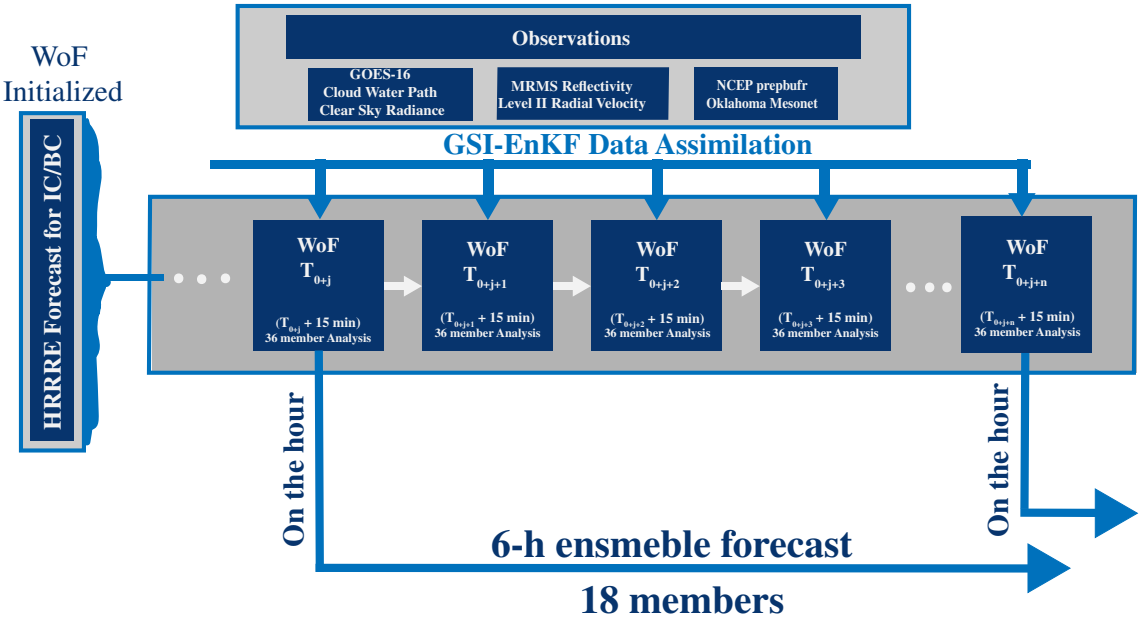

FIGURE 3 The schematic of the WoFS experiments [Colour figure can be viewed at wileyonlinelibrary.com]

TABLE 2 The WoFS experiment timeline for the three LTC events (Aug, Sep, Oct: August, September, October)

Name	Experiment type	WoFS DA cycle duration	0–6 hr WoFS ensemble forecasts (initialized hourly)
Harvey (2017)	Retrospective	1800 UTC 25 Aug–1200 UTC 26 Aug	0000 UTC 26 Aug–1200 UTC 26 Aug
Florence (2018)	Real time	1800 UTC 13 Sep–1200 UTC 14 Sep, 1800 UTC 14 Sep–0400 UTC 15 Sep	1900 UTC 13 Sep–1200 UTC 14 Sep, 1900 UTC 14 Sep–0400 UTC 15 Sep
Michael (2018)	Real time	1600 UTC 10 Oct–0400 UTC 11 Oct	1800 UTC 10 Oct–0400 UTC 11 Oct

time and 1, 3 and 6 hr forecasts thereafter with observed MRMS reflectivity contour overlaid at each forecast time provided for reference. For *Harvey*, high probabilities (>50%) of reflectivity exceeding 20 dBZ are comparable to observations with several small-scale differences apparent. For the 3 and 6 hr forecast times, there appears to be a southwest bias in reflectivity compared to observations indicating the forecast storm motion is somewhat too slow (Figure 5c,d). *Harvey* was embedded in a complex environment that did not favour a consistent storm motion. These environments are naturally more sensitive to model uncertainties and any biases or errors in the system are more likely to be apparent. However, WoFS accurately predicts the dissipation of precipitation in southern LA by 0900 UTC (Figure 5d). WoFS forecasts generated for *Florence* are somewhat less accurate, as the rain-band structure forecast by WoFS diverges from observed reflectivity after 1 hr with ensemble spread becoming quite extreme after 6 hr (Figure 5e–h). In contrast, WoFS performance with *Michael* was excellent during the 6 hr forecast following landfall (Figure 5i–l). High probabilities of reflectivity greater than 20 dBZ almost perfectly match observations out to 0000 UTC, with very few false alarms evident outside of *Michael*'s path. Hurricane *Michael*'s storm motion and eventual recurvature were well forecast due to an excellent environmental analysis by the model. An excellent representation of the environment combined with rain-band location and intensity provided through the data assimilation cycling resulted in a good forecast of the banding placement out to at least 6 hr.

4.2 | LTC rainfall

Comparison of observed and predicted reflectivity generally showed positive results, but verifying predicted rainfall against measurements provides a more accurate assessment of WoFS skill for LTC-induced flash flooding. For rainfall verification, the NCEP Stage IV (Lin and Mitchell, 2005) 6 hr accumulated rainfall analysis is used. The Stage IV analyses are produced from the regional hourly/6-hourly multi-sensor (radar and gauges) and are mosaicked into a national product. Some manual quality controls are done on the data. The 6 hr analysis Stage

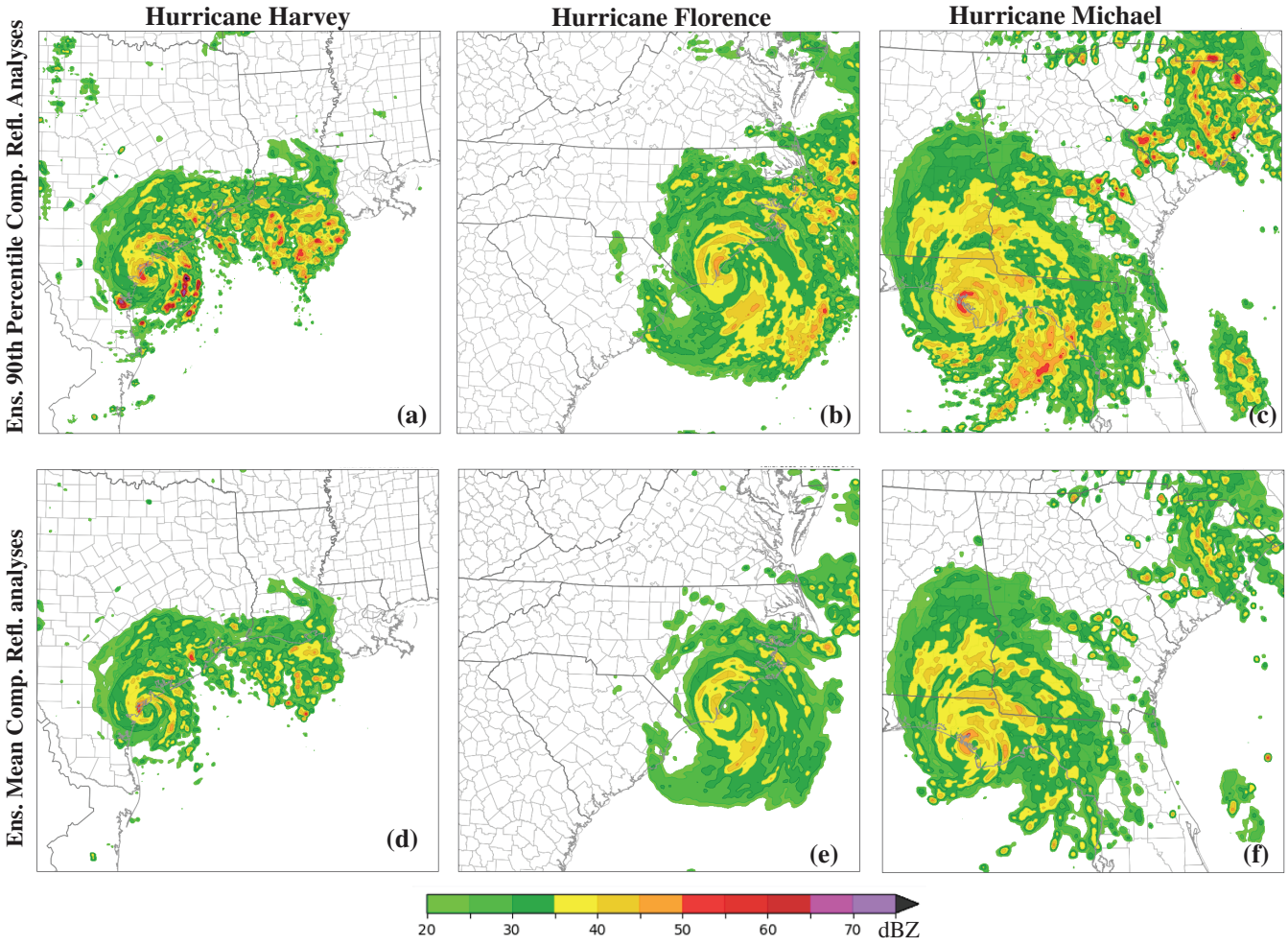

FIGURE 4 The WoFS ensemble analyses 90th percentile and mean of composite reflectivity (dBZ) near the time of landfall for (a,d) *Harvey* (26 August 2017 at 0300 UTC), (b,e) *Florence* (14 September 2018 at 1100 UTC), and (c,f) *Michael* (10 October 2018 at 1800 UTC) [Colour figure can be viewed at wileyonlinelibrary.com]

IV is compared against forecast rainfall during three forecast periods for each hurricane. Two forecast products are shown. The first is the 90th percentile of predicted rainfall, which represents a "reasonable" worst-case scenario and is calculated at each grid point as the value where 90% of ensemble members predict a lower rainfall total. The second is the probability of rainfall greater than 25.4 mm (1 in) to assess the overall coverage of heavy rainfall.

Figure 6 shows 6 hr accumulated rainfall forecasts initiated at 0000, 0600 and 1200 UTC 27 August covering the period during and after landfall of Hurricane *Harvey*. WoFS reasonably forecasts heavy precipitation produced within the inner core and with the primary rain band to the northeast. In particular, the 90th percentile forecasts (Figure 6d–f) generate the areas of maximum precipitation that correspond well with the locations and magnitude of maximum precipitation areas from observations. Probabilistic forecasts (Figure 6g–i) additionally show that the highest likelihoods of heavy precipitation correspond well with observations. The NOAA NWS *Storm Data* (NOAA, 2018) flood and flash-flood reports between 1200 and 1800 UTC 26 August 2017 are present within the primary rain band and are located near the areas of maximum predicted rainfall, though a small northeastward bias in the forecast exists at this time (Figure 6c,f,i). The NWS *Storm Data* are official publications with records of the occurrence of significant weather phenomena that cause fatalities, injuries and significant property damage. The NWS collect the information from a variety of sources including but not limited to county, state and federal emergency management offices, sky-warn spotters, NWS damage surveys, local law enforcement offices, newspaper clipping services, the insurance industry and the general public. There are other differences between observations and WoFS forecasts to note. First, WoFS over-forecasts precipitation along the upper TX and LA coastal areas, which corresponds to the forecast reflectivity bias. Second, the extent of forecast rainfall associated with the primary rain

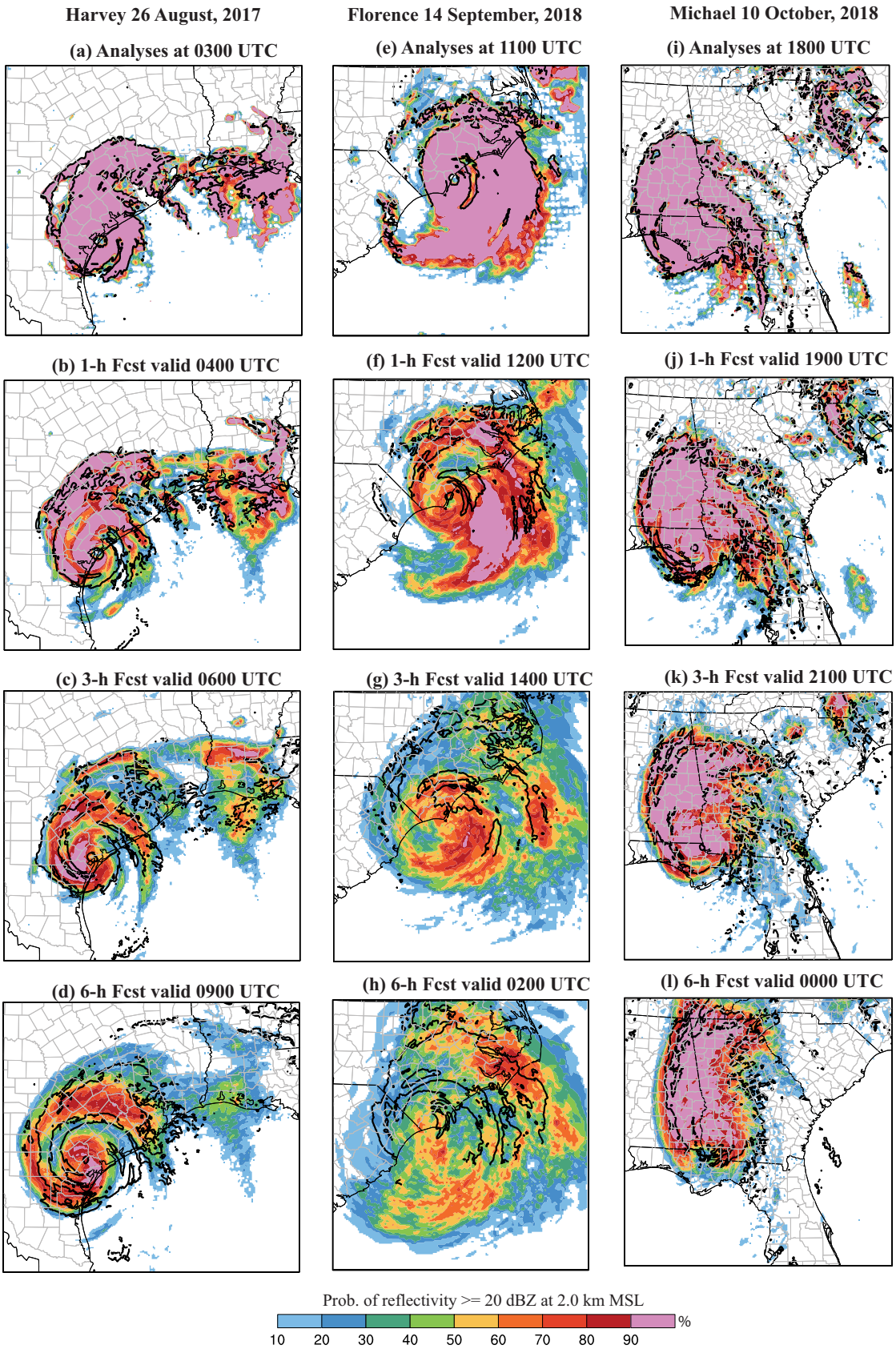

FIGURE 5 The ensemble probability of reflectivity greater than 20 dBZ (colours, 10% increment) at low level (2 km above mean sea level) from the analyses (a,e,i) at the time of landfall and 1 hr (b,f,j), 3 hr (c,g,k) and 6 hr (d,h,l) forecasts from hurricanes *Harvey* (left column), *Florence* (middle column) and *Michael* (right column). The thick black contour overlaid is the observed 20 dBZ reflectivity contour. The portion of the domain covers the landfall area [Colour figure can be viewed at wileyonlinelibrary.com]

band does not extend as far inland into TX as observed for all forecast periods. This is likely a result of the slower movement of the hurricane in the model compared to its observed speed.

Rainfall forecasts initiated at 1200, 2100 and 0300 UTC 14–15 September 2018 for hurricane *Florence* were somewhat less accurate (Figure 7). The forecasts overpredict the size of the tropical cyclone and the area between the eye and rain bands is too large in each forecast. Overall, the weakening inner core and strengthening rain-band features are correctly forecast, but both the magnitudes and coverage differ significantly for the forecasts initiated at 1200 UTC (Figure 7a,d,g). At this forecast time, both the magnitude and spatial extent of maximum rainfall do not correspond well with either rainfall measurements or locations of NWS *Storm Data* flood reports. However, the advantage of continuous cycling of the data assimilation system is evident in improved forecasts initiated at 2100 and 0300 UTC 15–16 September 2018. The areas of heavy rainfall are well forecast for these two periods, especially in the onshore flow in eastern NC (Figure 7e,f,h,i). By 0300 UTC, the forecast becomes excellent with the highest probabilities of 25.4 mm rainfall matching very well with Stage IV rainfall estimates. The 90th percentile total precipitation amounts overestimate actual rainfall amounts in some areas, but this is not surprising as this product is intended to provide a worst-case scenario for heavy rainfall. Interestingly, many NWS *Storm Data* heavy rainfall reports between 0300 and 0900 UTC occur in areas where little precipitation was observed. It is likely that some of these reports are delayed and represent the heavy rainfall that occurred over this region prior to 0300 UTC.

Rainfall forecasts for Hurricane *Michael* were excellent both during and well after landfall (Figure 8). Observed 6 hr rainfall in excess of 76.2 mm (3 in) was produced by eyewall and surrounding convection in a swath from the Florida panhandle into southern Alabama (AL) and GA between 1800 and 0000 UTC 10–11 October 2018 with many NWS *Storm Data* heavy rain reports along and east of this swath (Figure 8a). Heavy precipitation continued northward into GA and slowly decreased in intensity with smaller areas of heavy rain and fewer reports by the 0400–1000 UTC time period (Figure 8c). For all three forecast periods, the placement and magnitude of the heaviest precipitation was accurately forecast as well as the overall coverage of 25.4 mm or greater rainfall (Figure 8d–i). The largest difference between WoFS forecasts and observations occurs during the 0400–1000 UTC forecast period where an area of observed ~25.4 mm precipitation was not forecast by most members of WoFS (Figure 8i). Investigation of this anomaly showed that the boundary conditions used in this run were too dry, resulting in a low bias in precipitation along the western edge of the domain at later forecast times (not shown).

Qualitatively, WoFS does a reasonable job forecasting both the intensity and coverage of heavy rainfall. It is also important to assess these forecasts in a quantitative manner. Ensemble fractions skill score (eFSS: Duc *et al.*, 2013) for 25.4 mm (1.0 in), 50.8 mm (2.0 in), 76.2 mm (3.0 in) and 101.6 mm (4.0 in) accumulated rainfall thresholds for 3 and 6 hr precipitation forecasts were computed for each hurricane (Figure 9). The eFSS was computed over 3 or 6 hr ensemble forecast periods initiated hourly for all the forecast hours as in Table 2 (last column) and aggregated over each forecast set and ensemble member. The eFSS was also computed as a function of neighbourhood search radius with 0 km representing a pure grid-point comparison up to radii of 36 km (12 grid points). For all hurricanes, eFSS generally decreases as the precipitation threshold increases for both 0–3 and 0–6 hr forecasts. The eFSS is a measure of the spatial accuracy of the precipitation forecasts. The 0–6 hr accumulated precipitation forecast generally produces higher eFSS compared to the 0–3 hr accumulation period partially due to the smaller-scale features being averaged out to some degree in the later forecast period. For all hurricanes, eFSS increases as neighbourhood radius increases, which would be expected as small-scale spatial displacements between observed and forecast precipitation no longer have a negative impact on skill.

4.3 | LTC low-level mesocyclones

In addition to predicting the intense rainfall from LTCs, WoFS is also able to predict rotation associated with supercells present in the rain bands (Jones *et al.*, 2019). LTCs have historically produced many tornadoes due to the very high low-level wind shear present within the rain bands, particularly in the right-front quadrant of the storm (Edwards, 2012). WoFS was designed to detect storm rotational characteristics that can be used as a proxy for tornadoes (Yussouf *et al.*, 2013a; 2015) and its application to LTCs is a natural evolution of this capability. For *Harvey*, *Florence* and *Michael*, WoFS generated high forecast probabilities of low-level (0–2 km above ground level) vertical vorticity at 2 hr lead time which is up to 1 hr prior to NWS *Storm Data* reported tornadoes (Figure 10). In the cases of *Harvey* and *Florence*, the highest probabilities corresponded to the isolated tornado threat. *Michael* generated a couple of false alarms in addition to predicting the tornadic storm. Similar results were observed at other forecast times for other reported tornadoes (not shown).

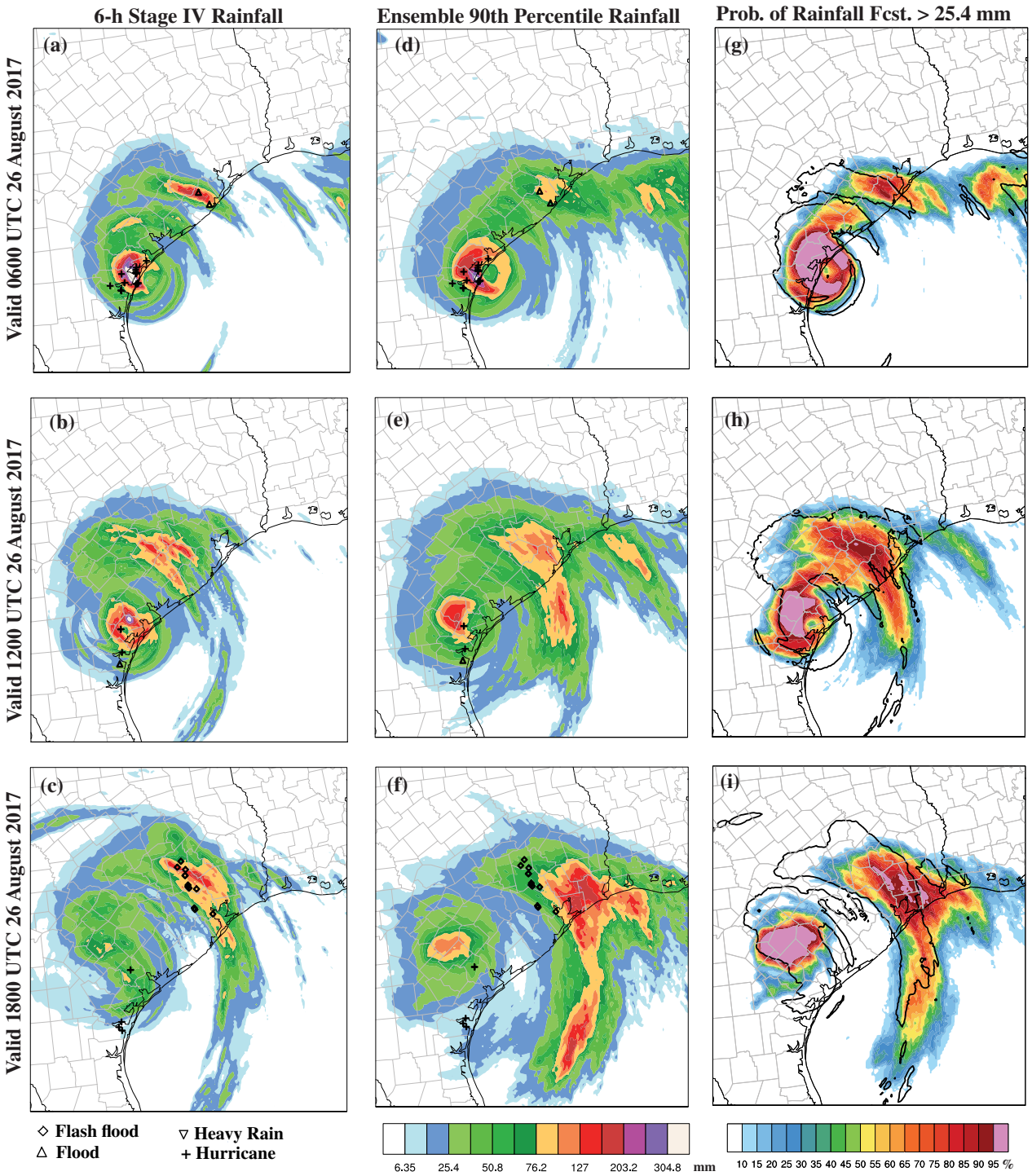

FIGURE 6 (a,b,c) The NCEP stage IV 6-hr rainfall totals overlaid with NWS reports of flash flood, flood, heavy rain and hurricane from *Storm Data* during the forecast time period, (d,e,f) ensemble 90th percentile, and (g,h,i) ensemble exceedance probabilities greater than 25.4 mm (1 in) of 0–6 hr accumulated rainfall forecasts initialized at 0000, 0600 and 1200 UTC 26 August 2017 for hurricane *Harvey*. Details are shown in the legends [Colour figure can be viewed at wileyonlinelibrary.com]

5 | SUMMARY AND CONCLUDING REMARKS

A convective-scale ensemble system with frequent 15 min DA cycling and sub-hourly forecast updates has been designed to improve short-term forecasts of tornadoes, flash flooding, damaging wind, and large hail. The system, known as the WoFS, can produce real-time, 0–6 hr probabilistic model guidance for the occurrence of weather hazards associated with individual storms.

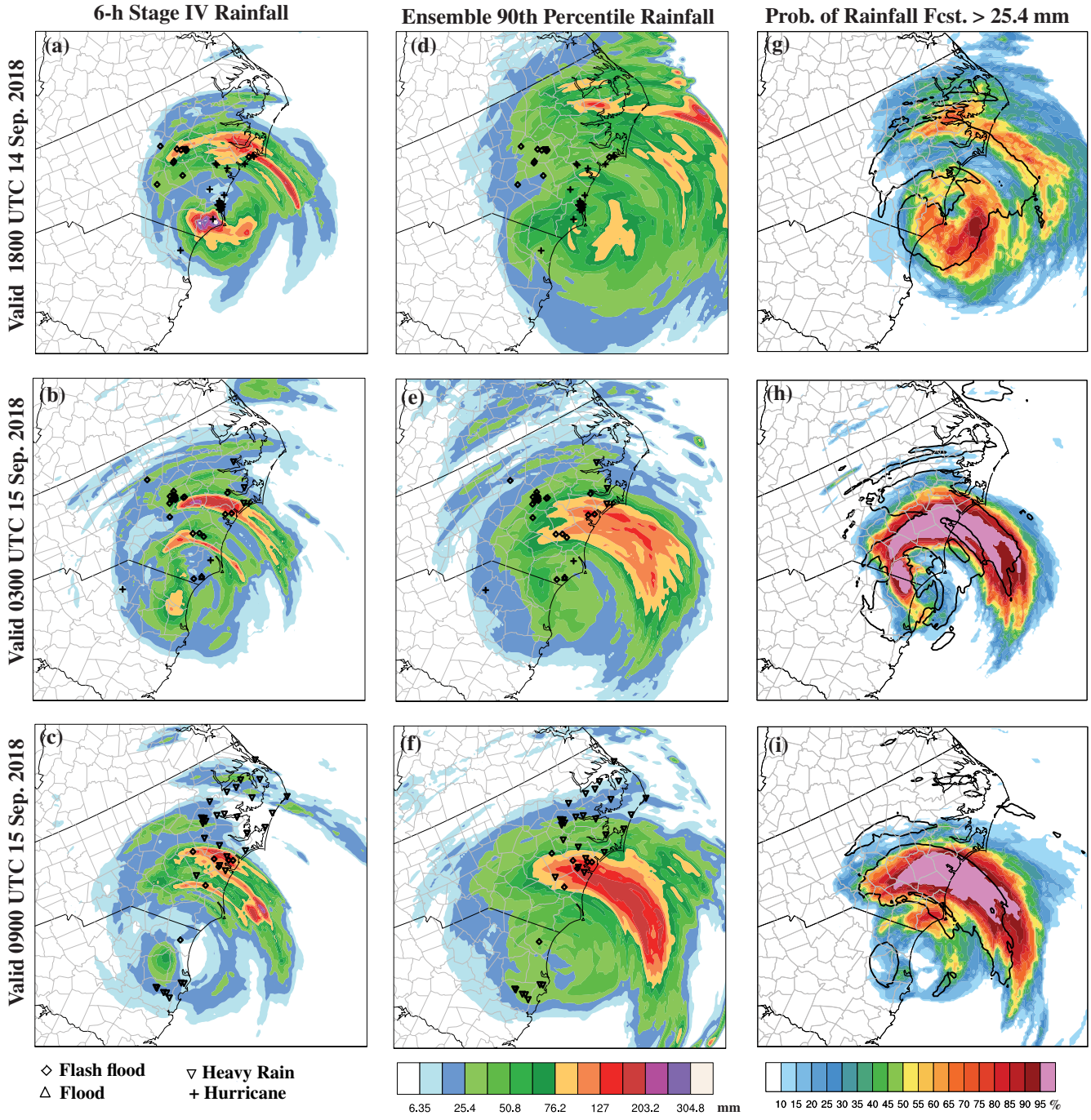

FIGURE 7 (a,b,c) The NCEP stage IV 6-hr rainfall totals overlaid with NWS reports from *Storm Data* during the forecast time period, (d,e,f) ensemble 90th percentile, and (g,h,i) ensemble exceedance probabilities of rainfall forecasts greater than 25.4 mm (1 in) of 0–6 hr accumulated rainfall forecasts initialized at 1200 and 2100 UTC 14 September and 0300 UTC 15 September 2018, for hurricane Florence [Colour figure can be viewed at wileyonlinelibrary.com]

This study investigates the application of WoFS for 0–6 hr ensemble prediction of intense rainfall from life-threatening LTCs. The goal of this study is not to forecast the track and intensity of the hurricane. Rather, the goal is to forecast the location and timing of intense rainfall associated with the tropical storm after it makes landfall.

The WoFS forecasts indicate that the three experiments are able to reproduce the LTC rain bands and rainfall with reasonable accuracy. The WoFS reflectivity analyses accurately represent the general location of the LTC during landfall. The ensemble-derived 90th percentile forecast indicated the severity, and the probabilistic products indicated the likelihood of the intense rainfall with good skill relative to the locations of the intense rainfall in Stage-IV analyses and NWS *Storm Data* flash flood and flood reports. The overall results underscore the need for

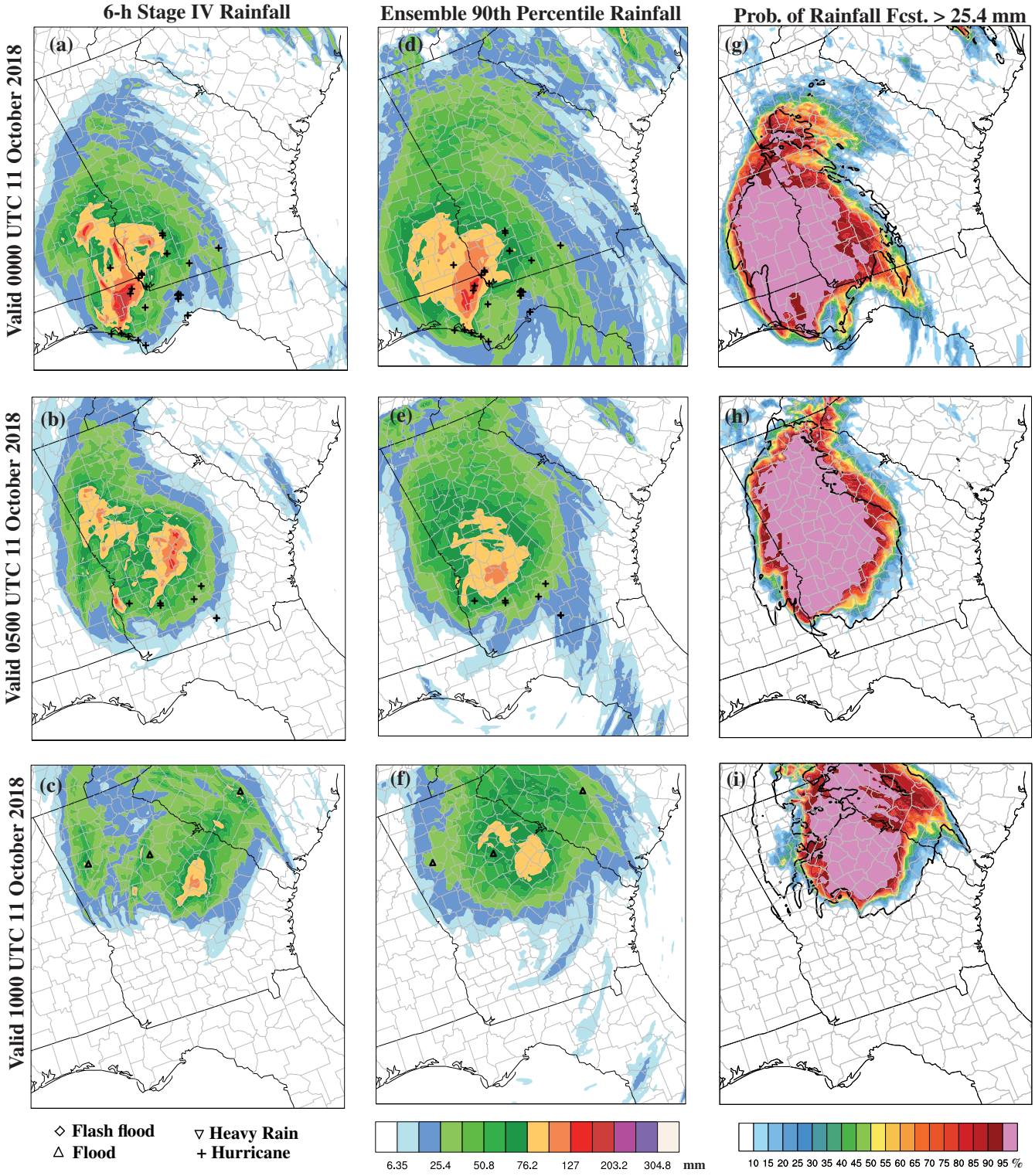

FIGURE 8 (a,b,c) the NCEP stage IV 6-hr rainfall totals overlaid with NWS reports from *Storm Data* during the forecast time period, (d,e,f) ensemble 90th percentile, and (g,h,i) ensemble exceedance probabilities greater than 25.4 mm (1 in) of 0–6 hr accumulated rainfall forecasts initialized at 1800 and 2300 UTC 10 October and 0400 UTC 11 October 2018 for hurricane *Michael* [Colour figure can be viewed at wileyonlinelibrary.com]

further improvement of the system to accurately represent the small-scale details of outer rain bands. The influence of boundary conditions due to the small WoFS domain, forecast uncertainty due to model error, insufficient model resolution, and the remaining unknowns in the underlying microphysical processes make accurate prediction of

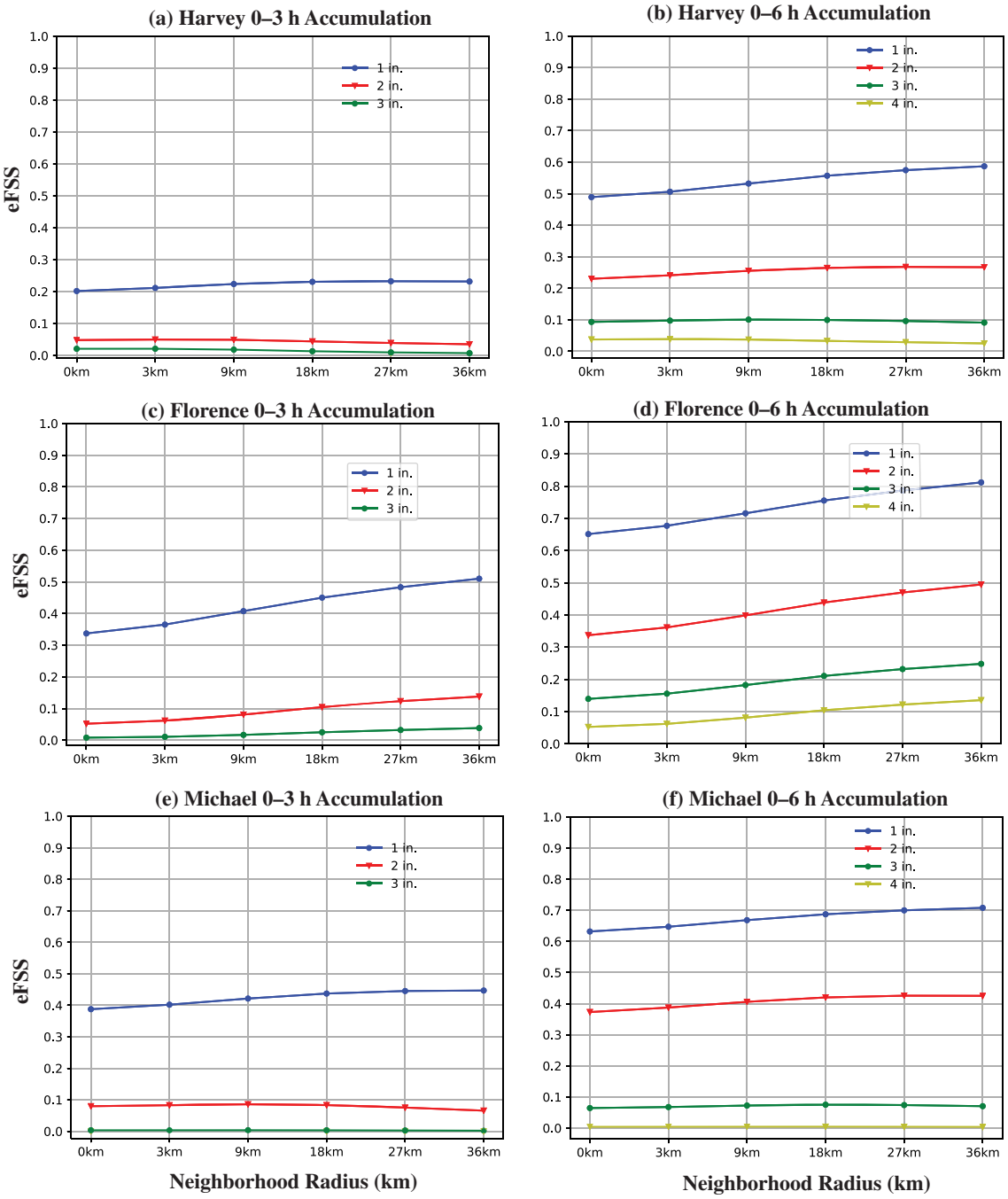

FIGURE 9 The 0–3 hr and 0–6 hr accumulated rainfall forecasts ensemble fractions skill score (eFSS) as a function of neighbourhood radius (km) for 25.4 mm (1.0 in; blue line), 50.8 mm (2.0 in; red line), 76.2 mm (3.0 in; green),101.6 mm (4.0 in; yellow). The aggregated eFSSs from the three cases are calculated over the domain presented in Figures 6–8 [Colour figure can be viewed at wileyonlinelibrary.com]

intense rainfall threat from LTC challenging. However, overall results indicate that a Warn-on-Forecast system can provide forecast information with greater continuity and specificity of the location and timing of hazards within the NWS watch and warning spatio-temporal scales and is aligned with NOAA's FACETs (Forecasting a Continuum of Environmental Threats: Rothfusz *et al.*, 2018) framework.

ACKNOWLEDGEMENTS

We thank Kent Knopfmeier for the real-time runs, David Dowell for providing the HRRRE data, and Jessie Choate for creating Figure 3. We appreciate the time and effort of two anonymous reviewers for providing constructive, thorough and insightful comments. Stage-IV data are provided by NCAR/EOL under the sponsorship of the National Science Foundation (https://

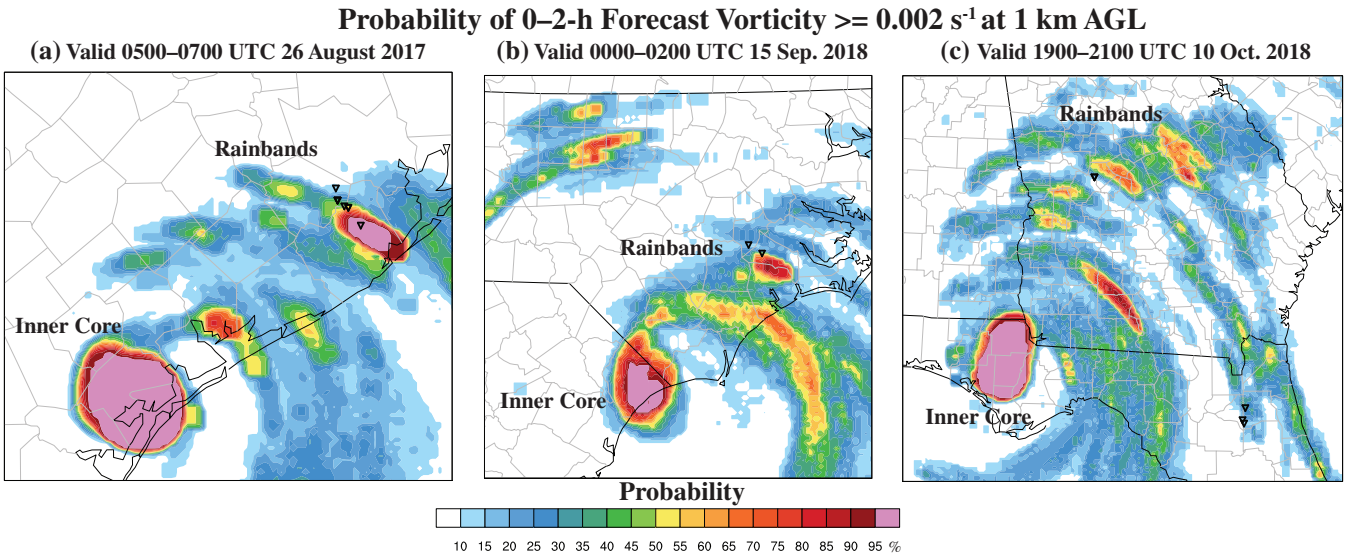

FIGURE 10 0–2 hr forecast ensemble probability of vorticity exceeding 0.002 s^{-1} (colours, 5% increment) at low level (1 km above ground level). The forecasts are initialized at (a) 0500 UTC 26 August 2017 for Hurricane *Harvey*, (b) 0000 UTC 15 September 2018 for Hurricane *Florence*, and (c) 1900 UTC 10 October 2018 for Hurricane *Michael*. The black triangles overlaid are the NWS tornado reports from *Storm Data* during the forecast period. The LTC inner core and tornadic rain bands are labelled [Colour figure can be viewed at wileyonlinelibrary.com]

data.eol.ucar.edu/). The supercomputer where all the experiments are run is maintained by Gerry Creager, Brett Morrow, Steven Fletcher and Robert Coggins. Funding for this research was provided by NOAA/NSSL FY 2018 Director's Discretionary Research Fund and NOAA-University of Oklahoma Cooperative Agreement No. NA11OAR4320072, US Department of Commerce.

ORCID

Nusrat Yussouf https://orcid.org/0000-0003-4998-1770

REFERENCES

Aksoy, A., Aberson, S.D., Vukicevic, T., Sellwood, K.J., Lorsolo, S. and Zhang, X. (2013) Assimilation of high-resolution tropical cyclone observations with an ensemble Kalman filter using NOAA/AOML/HRD's HEDAS: evaluation of the 2008–11 vortex-scale analyses. *Monthly Weather Review*, 141, 1842–1865. https://doi.org/10.1175/MWR-D-12-00194.1.

Alley, R.B., Emanuel, K.A. and Zhang, F. (2019) Advances in weather prediction. *Science*, 363, 342–344. https://doi.org/10.1126/science.aav7274.

Aon Benfield (2018) *Weather, climate and catastrophe insight: 2017 annual report*. Aon Report number: GDM05083, pp. 56. Available at: http://thoughtleadership.aonbenfield.com/Documents/20180124-ab-if-annual-report-weather-climate-2017.pdf [Accessed 20 September 2019].

Aon Benfield (2019) *Catastrophe insight*. Available at: http://www.aonbenfield.com/catastropheinsight [Accessed 20 September 2019].

Atallah, E.H., Bosart, L.F. and Aiyyer, A.R. (2007) Precipitation distribution associated with landfalling tropical cyclones over the eastern United States. *Monthly Weather Review*, 135, 2185–2206. https://doi.org/10.1175/MWR3382.1.

Beven II, J.L., Berg, R. and Hagen, A. (2019) *National Hurricane Center tropical cyclone report: Hurricane Michael*. Available at: https://www.nhc.noaa.gov/data/tcr/AL142018_Michael.pdf [Accessed 20 September 2019].

Blake, E.S. and Zelinsky, D.A. (2018) *National Hurricane Center tropical cyclone report: Hurricane Harvey*. Available at: https://www.nhc.noaa.gov/data/tcr/AL092017_Harvey.pdf [Accessed 22 September 2019].

Clark, R.A., Gourley, J.J., Flamig, Z.L., Hong, Y. and Clark, E. (2014) CONUS-wide evaluation of National Weather Service flash flood guidance products. *Weather and Forecasting*, 29, 377–392.

Czajkowski, J., Simmons, K. and Sutter, D. (2011) An analysis of coastal and inland fatalities in landfalling U.S. hurricanes. *Natural Hazards*, 59, 1513–1531. https://doi.org/10.1007/s11069-011-9849-x.

Czajkowski, J., Villarini, G., Michel-Kerjan, E. and Smith, J.A. (2013) Determining tropical cyclone inland flooding loss on a large-scale through a new flood peak ratio-based methodology. *Environmental Research Letters*, 8, 44–56. https://doi.org/10.1088/1748-9326/8/4/044056.

Dare, R.A., Davidson, N.E. and McBride, J.L. (2012) Tropical cyclone contribution to rainfall over Australia. *Monthly Weather Review*, 140, 3606–3619. https://doi.org/10.1175/MWR-D-11-00340.1.

Developmental Testbed Center. (2017a) *Gridpoint statistical interpolation user's guide version 3.6*. Available at: https://dtcenter.org/com-GSI/users/docs/ [Accessed 20 August 2019]. Pp. 158.

Developmental Testbed Center. (2017b) *Ensemble Kalman filter (EnKF) user's guide for version 1.2*. Available at: http://www.dtcenter.org/EnKF/users/docs/index.php [Accessed 20 August 2019]. Pp. 86.

Dowell, D.C., Alexander, C.R., Beck, J., Benjamin, S.G., Hu, M., Ladwig, T., Knopfmeier, K.H., Skinner, P.S. and Wheatley, D.M. (2016) Development of a high-resolution rapid refresh ensemble (HRRRE) for severe weather forecasting. [Preprints]

28th Conference on Severe Local Storms, Portland, OR. American Meteorology Society, p. 8B.2.

Duc, L., Saito, K. and Seko, H. (2013) Spatial–temporal fractions verification for high-resolution ensemble forecasts. *Tellus*, 65A, 18171. https://doi.org/10.3402/tellusa.v65i0.18171.

Edwards, R. (2012) Tropical cyclone tornadoes: a review of knowledge in research and prediction. *Electronic Journal of Severe Storms Meteorology*, 7, 1–61.

Emanuel, K.A. (2017) Assessing the present and future probability of Hurricane *Harvey*'s rainfall. *Proceedings of the National Academy of Sciences (PNAS) USA*, 114, 12681–12684. https://doi.org/10.1073/pnas.1716222114.

Houtekamer, P.L., Mitchell, H.L., Pellerin, G., Buehner, M., Charron, M., Spacek, L. and Hansen, B. (2005) Atmospheric data assimilation with an ensemble Kalman filter results with real observations. *Monthly Weather Review*, 133, 604–620.

Jones, T.A., Knopfmeier, K., Wheatley, D.M., Creager, G., Minnis, P. and Palikondo, R. (2016) Storm-scale data assimilation and ensemble forecasting with the NSSL experimental warn-on-forecast system. Part II: Combined radar and satellite data experiments. *Weather and Forecasting*, 31, 297–327. https://doi.org/10.1175/WAF-D-15-0107.1.

Jones, T.A., Skinner, P.S., Yussouf, N., Knopfmeier, K., Reinhart, A.E. and Dowell, D.C. (2019) Forecasting high-impact weather in landfalling tropical cyclones using a Warn-on-Forecast system. *Bulletin of the American Meteorological Society*, 100, 1405–1417. https://doi.org/10.1175/BAMS-D-18-0203.1.

Jones, T.A., Wang, X., Skinner, P., Johnson, A. and Wang, Y. (2018) Assimilation of GOES-13 imager clear-sky water vapor (6.5 μm) radiances into a Warn-on-Forecast system. *Monthly Weather Review*, 33(6), 1681–1708. https://doi.org/10.1175/MWR-D-17-0280.1.

Jonkman, S.N., Maaskant, B., Boyd, E. and Levitan, M.L. (2009) Loss of life caused by the flooding of New Orleans after Hurricane *Katrina*: analysis of the relationship between flood characteristics and mortality. *Risk Analysis*, 29, 676–698. https://doi.org/10.1111/j.1539-6924.2008.01190.

Kleist, D.T., Parrish, D.F., Derber, J.C., Treadon, R., Wu, W.-S. and Lord, S. (2009) Introduction of the GSI into the NCEP global data assimilation system. *Weather and Forecasting*, 24, 1691–1705.

Klotzbach, P.J., Bowen, S.G., Pielke, R.A., Jr. and Bell, M. (2018) Continental United States hurricane landfall frequency and associated damage: observations and future risks. *Bulletin of the American Meteorological Society*, 99, 1359–1376.

Leroux, M.-D., Wood, K., Elsberry, R.L., Cayanan, E., Hendricks, E.O., Kucas, M., Otto, P., Rogers, R., Sampson, C.R. and Yu, Z. (2018) Recent advances in research and forecasting of tropical cyclone track, intensity, and structure at landfall. *Tropical Cyclone Research and Review*, 7(2), 85–105.

Lin, Y. and Mitchell, K. (2005) The NCEP Stage II/IV hourly precipitation analyses: development and applications. [Preprint] *19th Conference on Hydrology, San Diego, CA*. American Meteorological Society.

Lu, X., Wang, X., Tong, M. and Tallapragada, V. (2017) GSI-based, continuously cycled, dual-resolution hybrid ensemble–variational data assimilation system for HWRF: system description and experiments with *Edouard* (2014). *Monthly Weather Review*, 145, 4877–4898. https://doi.org/10.1175/MWR-D-17-0068.1.

Mansell, E.R., Ziegler, C. and Bruning, E. (2010) Simulated electrification of a small thunderstorm with two-moment bulk microphysics. *Journal of Atmospheric Science*, 67, 171–194. https://doi.org/10.1175/2009JAS2965.1.

Meyer, R.J., Baker, E.J., Broad, K.F., Czajkowski, J. and Orlove, B. (2014) The dynamics of hurricane risk perception: real-time evidence from the 2012 Atlantic hurricane season. *Bulletin of the American Meteorological Society*, 95, 1389–1404. https://doi.org/, https://doi.org/10.1175/BAMS-D-12-00218.1.

NOAA. (2018) *Storm data preparation*. National Weather Service Instruction 10-1605, pp. 109. Available at: http://www.weather.gov/directives/sym/pd01016005curr.pdf [Accessed 25 September 2019.

Peduzzi, P., Chatenou, B., Dao, H., De Bono, A., Herold, C., Kossin, J., Mouton, F. and Nordbeck, O. (2012) Global trends in tropical cyclone risk. *Nature Climate Change*, 2, 289–294. https://doi.org/10.1038/nclimate1410.

Pielke Jr, R.A. and Pielke, R.A., Sr. (1997) *Hurricanes: Their nature and impacts on society*. England: John Wiley and Sons.

Rappaport, E.N. (2000) Loss of life in the United States associated with recent Atlantic tropical cyclones. *Bulletin of the American Meteorological Society*, 81, 2065–2073. https://doi.org/10.1175/1520-0477(2000)081<2065:LOLITU>2.3.CO;2.

Rappaport, E.N. (2014) Fatalities in the United States from Atlantic tropical cyclones: new data and interpretation. *Bulletin of the American Meteorological Society*, 95, 341–346. https://doi.org/10.1175/BAMS-D-12-00074.1.

Rappaport, E.N. and Blanchard, B.W. (2016) Fatalities in the United States indirectly associated with Atlantic tropical cyclones. *Bulletin of the American Meteorological Society*, 97(7), 1139–1148.

Rothfusz, L.P., Schneider, R., Novak, D., Klockow-McClain, K.E., Gerard, A., Karstens, C., Stumpf, G. and Smith, T. (2018) FACETs: a proposed next-generation paradigm for high-impact weather forecasting. *Bulletin of the American Meteorological Society*, 99, 2025–2043. https://doi.org/10.1175/BAMS-D-16-0100.1.

Simpson, R.H. and Riehl, H. (1981) *The Hurricane and its Impact*. Baton Rouge, LA: Louisiana State University Press.

Skamarock, W.C., Klemp, J.B., Dudhia, J., Gill, D.O., Barker, D.M., Duda, M.G., Huang, X.-Y., Wang, W. and Powers, J.G. (2008) *A description of the advanced research WRF version 3*. NCAR Technical Note NCAR/TN-475+STR, pp. 113.

Skinner, P.S., Wheatley, D.M., Knopfmeier, K.H., Reinhart, A.E., Choate, J.J., Jones, T.A., Creager, G.J., Dowell, D.C., Alexander, C.R., Ladwig, T.T., Wicker, L.J., Heinselman, P.L., Minnis, P. and Palikonda, R. (2018) Object-based verification of a prototype warn-on-forecast system. *Weather and Forecasting*, 33, 1225–1250.

Skinner, P.S., Wicker, L.J., Wheatley, D.M. and Knopfmeier, K.H. (2016) Application of two spatial verification methods to ensemble forecasts of low-level rotation. *Weather and Forecasting*, 31, 713–735.

Smirnova, T.G., Brown, J.M., Benjamin, S. and Kenyon, J. (2016) Modifications to the rapid update cycle land surface model (RUC LSM) available in the weather research and forecasting (WRF) model. *Monthly Weather Review*, 144, 1851–1865. https://doi.org/10.1175/MWR-D-15-0198.1.

Smith, T.M., Lakshmanan, V., Stumpf, G.J., Ortega, K.L., Hondl, K., Cooper, K., Calhoun, K.M., Kingfield, D.M., Manross, K.L., Toomey, R. and Brogden, J. (2016) Multi-radar multi-sensor (MRMS) severe weather and aviation products: initial operating

capabilities. *Bulletin of the American Meteorological Society*, 97(9), 1617–1630. https://doi.org/10.1175/BAMS-D-14-00173.1.

Stensrud, D.J., Wicker, L.J., Xue, M., Dawson, D.T., II, Yussouf, N., Wheatley, D.M., Thompson, T.E., Snook, N.A., Smith, T.M., Schenkman, A.D., Potvin, C.K., Mansell, E.R., Lei, T., Kuhlman, K.M., Jung, Y., Jones, T.A., Gao, J., Coniglio, M.C., Brooks, H.E. and Brewster, K.A. (2013) Progress and challenges with Warn-on-Forecast. *Atmospheric Research*, 123, 2–16.

Stensrud, D.J., Xue, M., Wicker, L.J., Kelleher, K.E., Foster, M.P., Schaefer, J.T., Schneider, R.S., Benjamin, S.G., Weygandt, S.S., Ferree, J.T. and Tuell, J.P. (2009) Convective-scale warn-on-forecast system: a vision for 2020. *Bulletin of the American Meteorological Society*, 90, 1487–1499.

Stewart, S.R. and Berg, R. (2019) *National Hurricane Center tropical cyclone report: Hurricane Florence*. Available at: https://www.nhc.noaa.gov/data/tcr/AL062018_Florence.pdf [Accessed 25 September, 2019].

Tong, M., Sippel, J.A., Tallapragada, V., Liu, E., Kieu, C., Kwon, I., Wang, W., Liu, Q., Ling, Y. and Zhang, B. (2018) Impact of assimilating aircraft reconnaissance observations on tropical cyclone initialization and prediction using operational HWRF and GSI ensemble–variational hybrid data assimilation. *Monthly Weather Review*, 146, 4155–4177. https://doi.org/10.1175/MWR-D-17-0380.1.

Wheatley, D.M., Knopfmeier, K.H., Jones, T.A. and Creager, G.J. (2015) Storm-scale data assimilation and ensemble forecasting with the NSSL experimental Warn-on-Forecast system. Part I: Radar data experiments. *Weather and Forecasting*, 30, 1795–1817.

Whitaker, J.S., Hamill, T.M., Wei, X., Song, Y. and Toth, Z. (2008) Ensemble data assimilation with the NCEP global forecast system. *Monthly Weather Review*, 136, 463–482. https://doi.org/10.1175/2007MWR2018.1.

WMO. (2017) HIWeather: a 10-year research project. *WMO Bulletin*, 66(2) Available at: https://public.wmo.int/en/resources/bulletin/hiweather-10-year-research-project. [Accessed 3 May 2019].

Yussouf, N., Dowell, D.C., Wicker, L.J., Knopfmeier, K. and Wheatley, D.M. (2015) Storm-scale data assimilation and ensemble forecasts for the 27 April 2011 severe weather outbreak in Alabama. *Monthly Weather Review*, 143, 3044–3066.

Yussouf, N., Gao, J., Stensrud, D.J. and Ge, G. (2013b) The impact of mesoscale environmental uncertainty on the prediction of a tornadic supercell storm using ensemble data assimilation approach. *Advances in Meteorology*, 2013, 1–15.

Yussouf, N., Kain, J.S. and Clark, A.J. (2016) Short-term probabilistic forecasts of the 31 May 2013 Oklahoma tornado and flash flood event using a continuous-update-cycle storm-scale ensemble system. *Weather and Forecasting*, 31, 957–983.

Yussouf, N. and Knopfmeier, K.H. (2019) Application of Warn-on-Forecast System for flash-flood producing heavy convective rainfall events. *Quarterly Journal of the Royal Meteorological Society*, 145, 2385–2403. https://doi.org/10.1002/qj.3568.

Yussouf, N., Mansell, E.R., Wicker, L.J., Wheatley, D.M. and Stensrud, D.J. (2013a) The ensemble Kalman filter analyses and forecasts of the 8 May 2003 Oklahoma City tornadic supercell storm using single and double moment microphysics schemes. *Monthly Weather Review*, 141, 3388–3412.

Zhang, F., Minamide, M., Nystrom, R.G., Chen, X., Lin, S.J. and Harris, L.M. (2019) Improving *Harvey* forecasts with next-generation weather satellites. *Bulletin of the American Meteorological Society*, 100, 1217–1222. https://doi.org/10.1175/BAMS-D-18-0149.1.

Zhang, F. and Weng, Y. (2015) Predicting hurricane intensity and associated hazards: a five-year real-time forecast experiment with assimilation of airborne Doppler radar observations. *Bulletin of the American Meteorological Society*, 96, 25–33. https://doi.org/10.1175/BAMS-D-13-00231.1.

Zhang, F., Weng, Y. and Kuo, Y.-H. (2010) Predicting typhoon *Morakot*'s catastrophic rainfall with a convection-permitting mesoscale ensemble system. *Weather and Forecasting*, 25, 1816–1825. https://doi.org/10.1175/2010WAF2222414.1.

How to cite this article: Yussouf N, Jones TA, Skinner PS. Probabilistic high-impact rainfall forecasts from landfalling tropical cyclones using Warn-on-Forecast system. *Q J R Meteorol Soc*. 2020;146:2050–2065. https://doi.org/10.1002/qj.3779